October 7, 1997

Peter Cheimets
Smithsonian Astrophysical Observatory
60 Garden Street, MS 5
Cambridge, MA 02138

Dear Peter:

This is the report on all of the HIREX analysis done to date, with corrections to the previous (and now obsolete) version dated 10/6/97. (Although there are still funds remaining, we are billing for this work, and will wait for word from you on what if anything else should be done.) We worked on the following design and analysis tasks:

- define a top level error budget for the mirror surfaces
- define a baseline off-axis configuration
- analyze the performance vs. field angle
- assess the feasibility of tilting the secondary to accomplish the pointing
- analyze the sensitivities to misalignments and define an alignment approach

We summarize the results from each of these tasks below.

I. Error budget

In order to define an error budget, we used our proprietary EENEAR computer program. EENEAR allows the user to assign statistical errors to the pupil of an optical system and analyze the point spread function and encircled energy. (EENEAR is related to the EEGRAZ program that was developed for and used in the AXAF program. Unlike EEGRAZ, which works only at grazing incidence, EENEAR works at all angles of incidence. As with EEGRAZ, there is no limitation on the magnitude of the surface errors compared with the radiation wavelength.)

In order to generate a useful set of parameters for EENEAR, we analyzed the published information on the one-dimensional Power Spectral Density (PSD) functions of the AXAF mirrors, since they were polished by Hughes Danbury Optical Systems (HDOS), which is also a good candidate to polish the HIREX mirrors. By looking at the power law falloff of the PSD for a typical hyperboloid and a typical paraboloid and averaging the results, we came up with a one-dimensional PSD whose magnitude varied as the spatial frequency raised to the (-2.55) power. The two-dimensional PSD, then, would vary as the spatial frequency raised to the (-3.55) power. We used such a PSD for our calculations, with a low frequency rolloff at one-half cycle per pupil radius. Specifically, the PSD has the form

$$PSD = A\,(f^2 + f0^2)^{(-3.55\,/\,2)}$$

where f is the magnitude of the two-dimensional spatial frequency, f0 is the low frequency rolloff, and the A-constant is adjusted to give the proper total rms surface error over all spatial frequencies. Figures 1-3 show the point spread function and encircled energy results of assigning 5, 10, and 15 Angstroms respectively to the pupil of the system, at a wavelength of 195 Angstroms. In each case, the point spread function and the encircled energy are compared with the diffraction limited case. After discussing these results with you, it seems that a total rms of something near 10-12 Angstroms would be appropriate. "Total" in this case means the root sum square of the primary, secondary, and tertiary mirror contributions. We assume that the largest portion of this would come from the aspherical primary mirror.

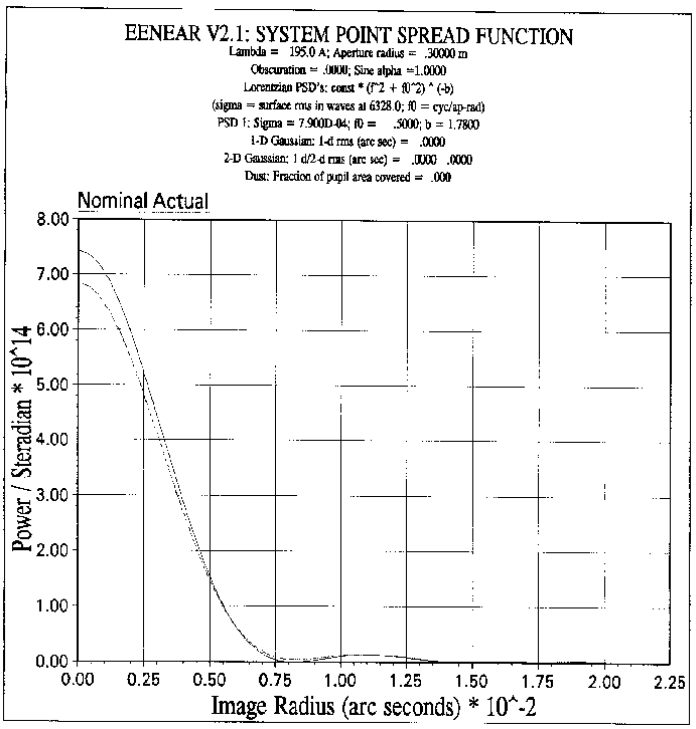

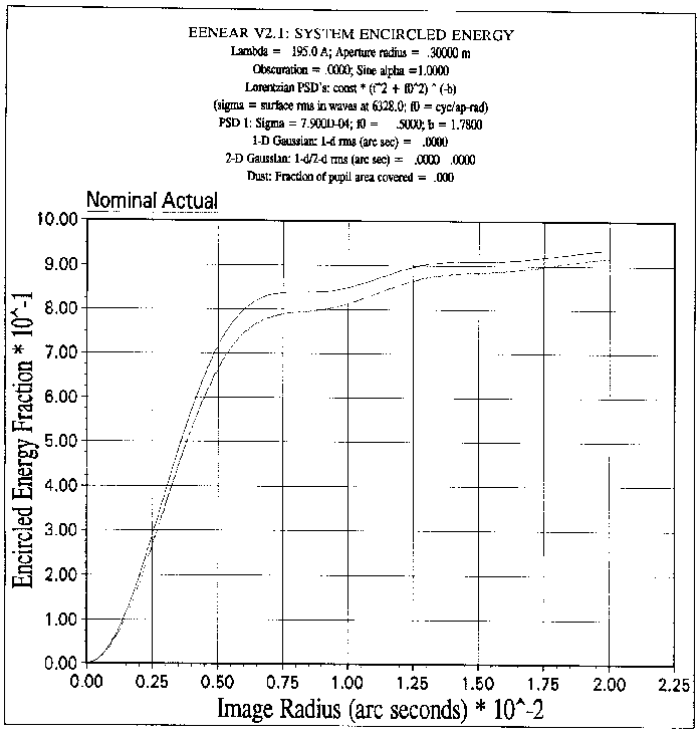

Figure 1. Point spread function and encircled energy for 5 Angstrom total surface rms.

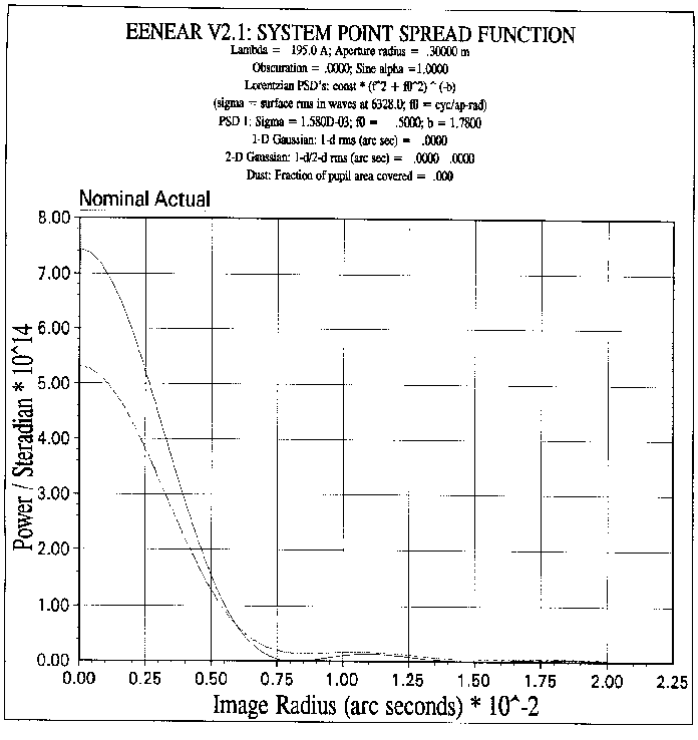

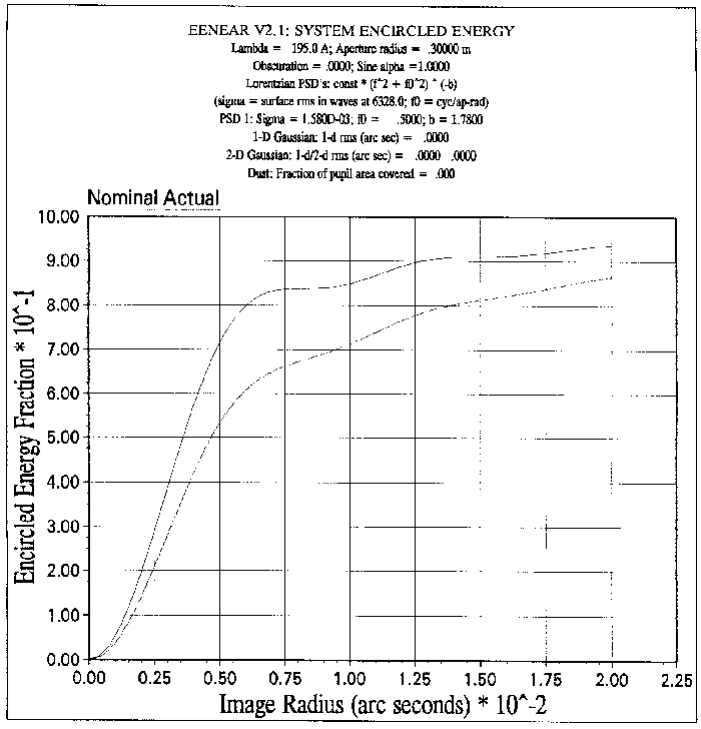

Figure 2. Point spread function and encircled energy for 10 Angstrom total surface rms.

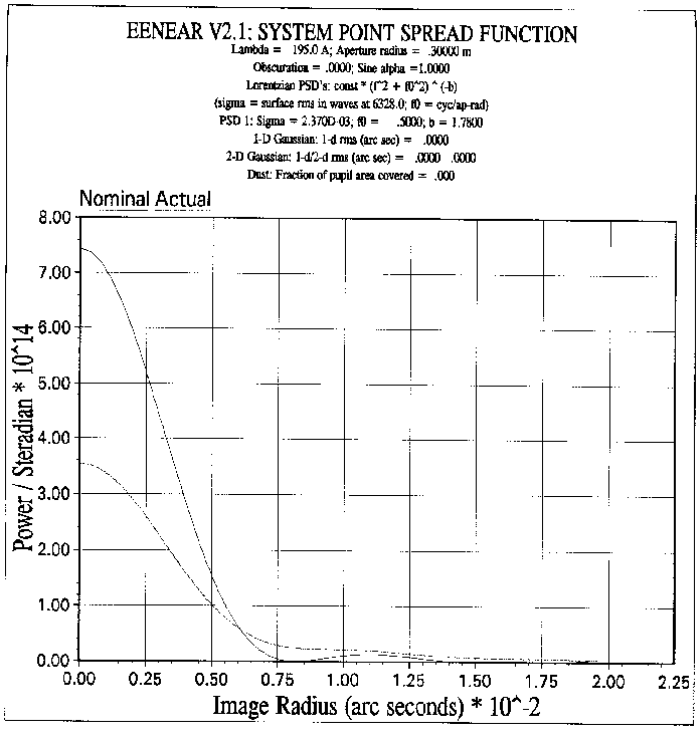

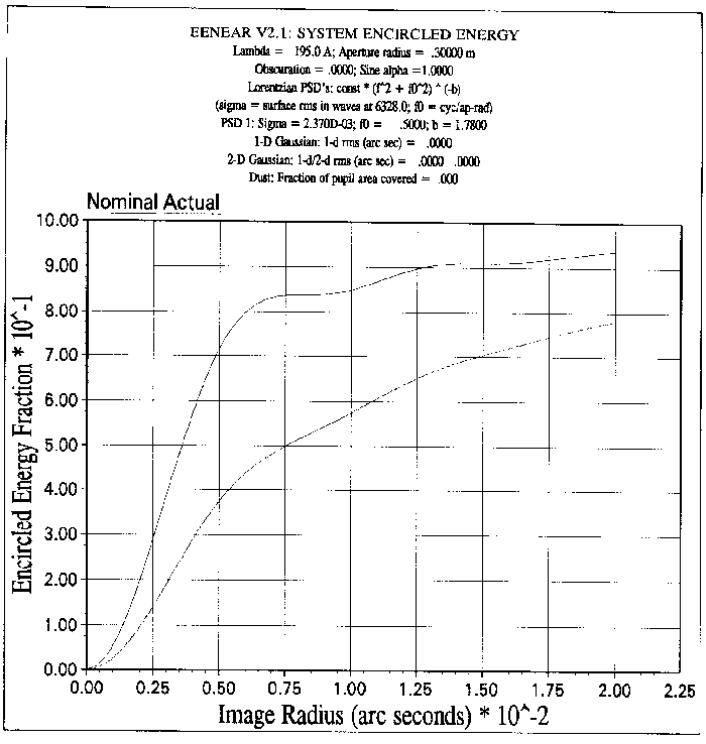

Figure 3. Point spread function and encircled energy for 15 Angstrom total surface rms.

II. Baseline off-axis configuration

We used the ZEMAX optical design program to design a baseline off-axis HIREX system. The aspherical primary mirror, which is also the aperture stop, is 600 mm in diameter, and the spherical secondary mirror is 97 mm in diameter. The separation between the two is 34357 mm. In order to assure that the sun's penumbra never falls on the primary mirror, we allowed for a separation of 300 mm between the edge of the secondary mirror and the edge of the centered incoming bundle of light. (Here, "centered" means the bundle coming from the center of the field of view. The direction of this center of field of view defines a sort of optical axis, even though the system as designed is not rotationally symmetric.) This separation guarantees that the penumbra never falls on the primary mirror, even when viewing the limb of the sun. Figure 4 shows a distorted view of the off-axis system, where the axial dimension has been shrunk compared to the lateral dimensions by a factor of ten. For comparison, Figure 5 shows the same type of view of the baseline on axis configuration.

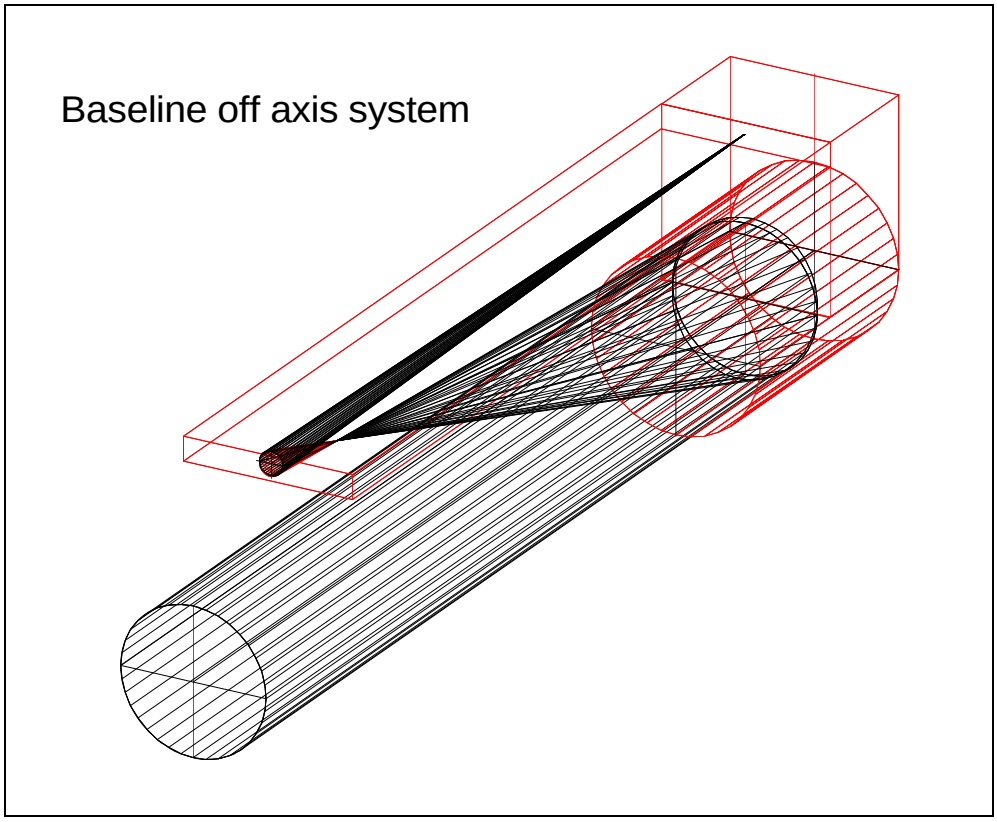

Figure 4. Distorted view of the baseline off-axis system.

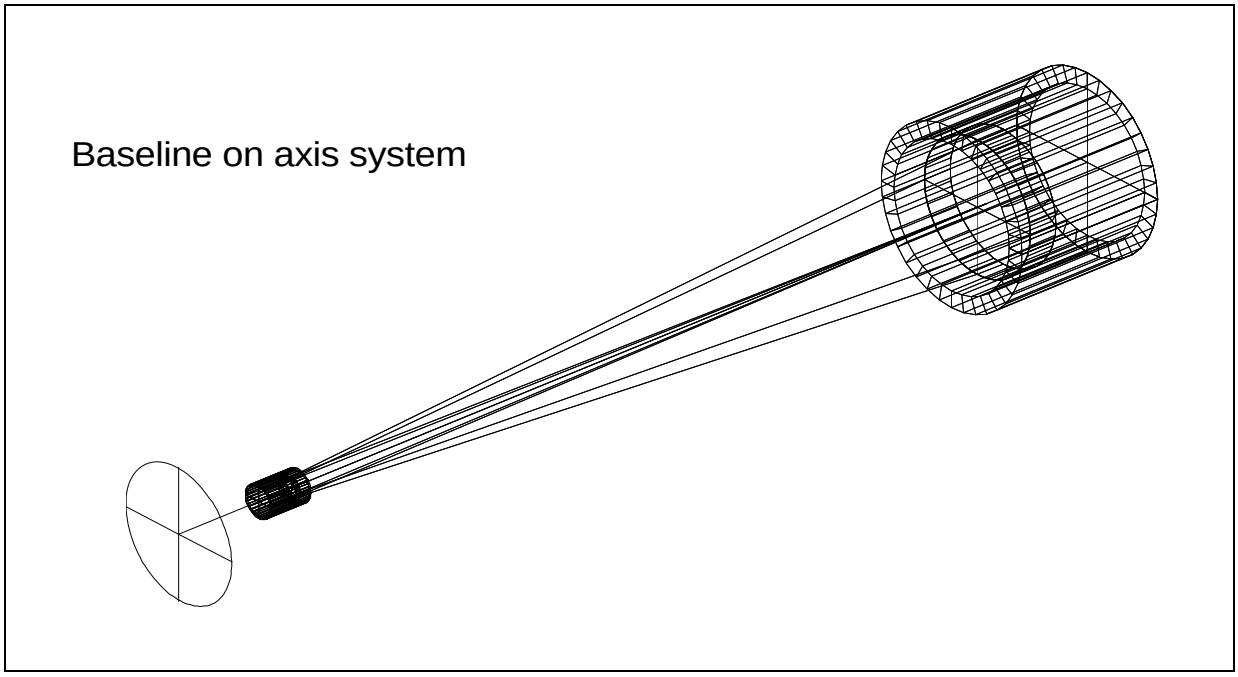

Figure 5. Distorted view of the baseline on-axis system.

Figure 6 is a printout from the ZEMAX program that shows all of the pertinent design information for the off-axis system. Note that the aspherizing of the primary mirror is limited to making it toroidal. Some comatic asphericity will need to be added, but it is not shown in Figure 6 as a Zernike deformation. There are thus three types of asphericity now assumed on the primary mirror. The first is spherical aberration, which simply means that a non-spherical conic section is being used. The second is astigmatism, which is needed because the mirrors are not being used at normal incidence, which in turn means that their tangential and sagittal apparent curvatures differ. The third is coma, which is the only other appreciable off-axis aberration. Table 1 lists these three types of asphericity, along with their peak-to-valley magnitudes. (There is some slight residual asphericity beyond these three types that would be added, but the peak-to-valley magnitude is only of the order of 0.003 micron.)

Type of asphericity	**Comment**	**Peak-to-valley magnitude (um)**
spherical aberration	corrects on-axis imaging	< 0.1
astigmatism	most basic off-axis aberration	0.8
coma	other non-negligible off-axis aberration	0.3

Table 1. Summary of the asphericities on the primary mirror.

```
System/Prescription Data

File : C:\ZEMAX\HIREX\offax2.ZMX
Title: OFFAX2 - Off axis, toroidal primary
Date : MON OCT 6 1997

GENERAL LENS DATA:

Surfaces        :               14
Stop            :                2
System Aperture : Entrance Pupil Diameter = 600
Ray aiming      : Off
Apodization     :Uniform, factor =   0.00000E+000
Eff. Focal Len. :       -243618.1 (in air)
Eff. Focal Len. :       -243618.1 (in image space)
Back Focal Len. :        35081.36
Total Track     :           35500
Image Space F/# :        406.0302
Para. Wrkng F/# :         404.589
Working F/#     :        402.9553
Obj. Space N.A. :    2.99999e-008
Stop Radius     :             300
Parax. Ima. Hgt.:         35.4314
Parax. Mag.     :               0
Entr. Pup. Dia. :             600
Entr. Pup. Pos. :           35000
Exit Pupil Dia. :        75.72189
Exit Pupil Pos. :       -30521.16
Field Type      : Angle in degrees
Maximum Field   :        0.008333
Primary Wave    :           0.017
Lens Units      :   Millimeters
Angular Mag.    :       -7.923732
```

Figure 6. ZEMAX output for off-axis system (page 1 of 4)

SURFACE DATA SUMMARY:

Surf	Type	Comment	Radius	Thickness	Glass	Diame
OBJ	STANDARD		Infinity	Infinity		
1	STANDARD		Infinity	35000		610.1
STO	STANDARD		Infinity	0		
3	COORDBRK		-	0	-	
4	TOROIDAL		-60064.86	0	MIRROR	
5	COORDBRK		-	0	-	
6	STANDARD		Infinity	-34357.14		600.0
7	COORDBRK		-	0	-	
8	STANDARD		7700.173	0	MIRROR	96.55
9	COORDBRK		-	0	-	
10	STANDARD		Infinity	34357.14		96.55
11	STANDARD		Infinity	500		869.8
12	STANDARD		Infinity	0		881.4
13	STANDARD		Infinity	0		881.4
IMA	STANDARD		Infinity			881.4

Figure 6. ZEMAX output for off-axis system (page 2 of 4)

```
SURFACE DATA DETAIL:

Surface OBJ     : STANDARD
Surface   1     : STANDARD
Surface STO     : STANDARD
Surface   3     : COORDBRK
 Decenter X     :                0
 Decenter Y     :                0
 Tilt About X   :            0.542
 Tilt About Y   :                0
 Tilt About Z   :                0
 Order          : Decenter then tilt
Surface   4     : TOROIDAL
 Rad of rev.    :        -60058.21
 Coeff on y^2   :                0
 Coeff on y^4   :                0
 Coeff on y^6   :                0
 Coeff on y^8   :                0
 Coeff on y^10  :                0
 Coeff on y^12  :                0
 Coeff on y^14  :                0
Surface   5     : COORDBRK
 Decenter X     :                0
 Decenter Y     :                0
 Tilt About X   :                0
 Tilt About Y   :                0
 Tilt About Z   :                0
 Order          : Decenter then tilt
Surface   6     : STANDARD
Surface   7     : COORDBRK
 Decenter X     :                0
 Decenter Y     :              325
 Tilt About X   :          -0.1251
 Tilt About Y   :                0
 Tilt About Z   :                0
 Order          : Decenter then tilt
Surface   8     : STANDARD
Surface   9     : COORDBRK
 Decenter X     :                0
 Decenter Y     :                0
 Tilt About X   :                0
 Tilt About Y   :                0
 Tilt About Z   :                0
 Order          : Decenter then tilt
Surface  10     : STANDARD
Surface  11     : STANDARD
Surface  12     : STANDARD
Surface  13     : STANDARD
Surface IMA     : STANDARD
```

Figure 6. ZEMAX output for off-axis system (page 3 of 4)

GLOBAL VERTEX COORDINATES, ORIENTATIONS, AND ROTATION/OFFSET MATRICES:
Reference Surface: 1

Surf	R11	R12	R13	X
	R21	R22	R23	Y
	R31	R32	R33	Z
1	1.000000	0.000000	0.000000	0.000000
	0.000000	1.000000	0.000000	0.000000
	0.000000	0.000000	1.000000	0.000000
2	1.000000	0.000000	0.000000	0.000000
	0.000000	1.000000	0.000000	0.000000
	0.000000	0.000000	1.000000	35000.000000
3	1.000000	0.000000	0.000000	0.000000
	0.000000	0.999955	-0.009460	0.000000
	0.000000	0.009460	0.999955	35000.000000
4	1.000000	0.000000	0.000000	0.000000
	0.000000	0.999955	-0.009460	0.000000
	0.000000	0.009460	0.999955	35000.000000
5	1.000000	0.000000	0.000000	0.000000
	0.000000	0.999955	-0.009460	0.000000
	0.000000	0.009460	0.999955	35000.000000
6	1.000000	0.000000	0.000000	0.000000
	0.000000	0.999955	-0.009460	0.000000
	0.000000	0.009460	0.999955	35000.000000
7	1.000000	0.000000	0.000000	0.000000
	0.000000	0.999974	-0.007276	649.988318
	0.000000	0.007276	0.999974	644.397224
8	1.000000	0.000000	0.000000	0.000000
	0.000000	0.999974	-0.007276	649.988318
	0.000000	0.007276	0.999974	644.397224
9	1.000000	0.000000	0.000000	0.000000
	0.000000	0.999974	-0.007276	649.988318
	0.000000	0.007276	0.999974	644.397224
10	1.000000	0.000000	0.000000	0.000000
	0.000000	0.999974	-0.007276	649.988318
	0.000000	0.007276	0.999974	644.397224
11	1.000000	0.000000	0.000000	0.000000
	0.000000	0.999974	-0.007276	399.998434
	0.000000	0.007276	0.999974	35000.627722
12	1.000000	0.000000	0.000000	0.000000
	0.000000	0.999974	-0.007276	396.360327
	0.000000	0.007276	0.999974	35500.614486
13	1.000000	0.000000	0.000000	0.000000
	0.000000	0.999974	-0.007276	396.360327
	0.000000	0.007276	0.999974	35500.614486
14	1.000000	0.000000	0.000000	0.000000
	0.000000	0.999974	-0.007276	396.360327
	0.000000	0.007276	0.999974	35500.614486

Figure 6. ZEMAX output for off-axis system (page 4 of 4)

III. Performance vs. field angle

We analyzed the performance as a function of field angle for both the on-axis and the off-axis configurations. In both cases, the only non-negligible aberrations were astigmatism and coma. The coma varies linearly with field angle in both cases. The astigmatism has a quadratic variation in both cases. However, in the off-axis case, the astigmatism also has a linear component to the variation because of the non-normal incidence. Naturally, we balanced these (by adding the toroidal asphericity to the primary mirror) to get zero astigmatism at the center of the field. However, the fact that both variations are present gives an asymmetry to the field performance in the tangential direction for the off-axis case. (In the sagittal direction, the on-axis and the off-axis cases should behave similarly.) Figure 7 shows the results for both cases, demonstrating that both the on-axis and the off-axis configurations easily give diffraction limited performance over the +/- 0.5 arc-minute field of view.

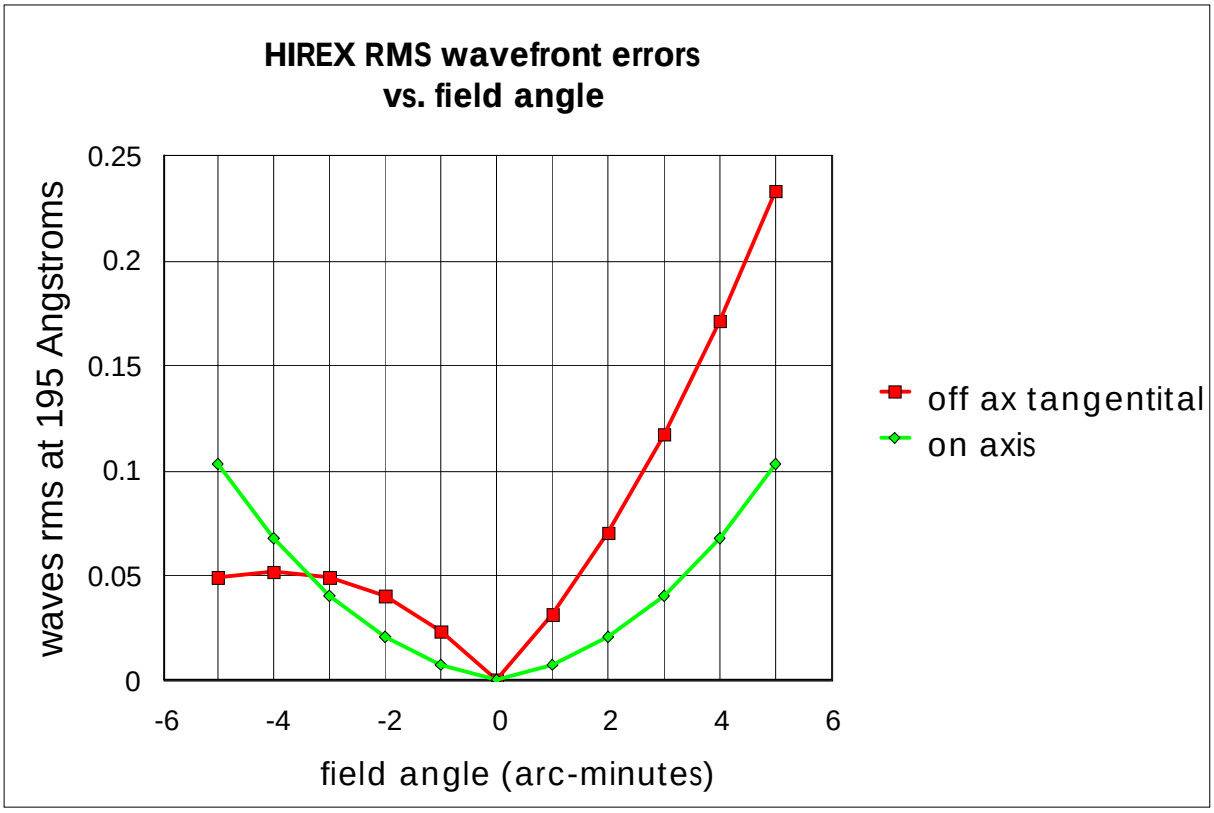

Figure 7. Performance vs. field angle for the on-axis and off-axis configurations.

IV. Tilting the secondary to accomplish pointing

We investigated whether it was feasible to tilt the secondary mirror to accomplish the pointing to different areas on the sun. We did this investigation strictly with the on-axis configuration. However, since the performance as a function of field angle was comparable for the on-axis and off-axis configurations, we expect that the point performance would also be comparable. In any case, for the on-axis configuration, we found that astigmatism varied quadratically and that coma varied linearly with the field angle after resteering the secondary mirror (just as they did in the more conventional analysis of the performance vs. field angle). Figure 8 summarizes the results, demonstrating that this approach can be used without significantly degrading performance out to a field angle of approximately 4 arc-minutes. (It is worth noting that the secondary mirror must be refocused after pointing. For a field angle of 15 arc-minutes, the required axial displacement is 1.1 mm. The displacement would vary quadratically with the field angle.) (Note: Figure 8 is revised since the 10/6/97 report, and the value of 1.1 mm for refocus is a corrected value.)

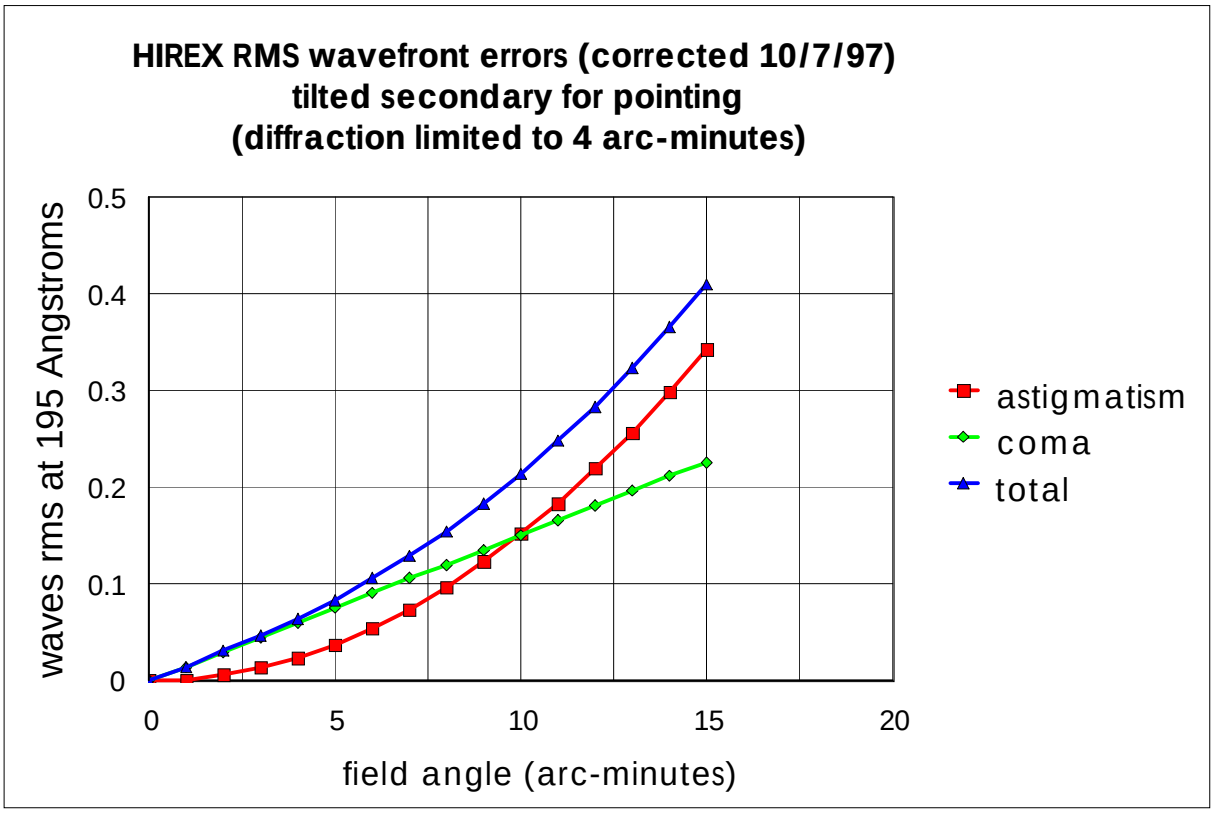

Figure 8. Performance as a function of field angle after steering the secondary mirror (on-axis configuration).

V. Alignment

Before defining the alignment tolerances, it is important first to discuss the alignment philosophy. Specifically, the primary mirror and the focal plane are to be considered a fixed assembly. This assembly would be put together and installed in the overall telescope using conventional optical shop surveying techniques. Typical tolerances would be a small fraction of the field of view - in other words, tolerances of arc-seconds or tens of arc-seconds would be sufficient, and these are easily achievable.

With the primary mirror and the focal plane permanently aligned and installed in the overall telescope, the only remaining important alignment is that of the secondary mirror. Since the secondary mirror is *spherical*, there is no tolerance on decenter - decenter is exactly the same as tilt. Therefore, there are only two tolerances - tilt and despace.

The despace tolerance can be gotten by using the standard criterion of quarter-wavelength peak-to-valley wavefront error. This criterion is equivalent to a depth of focus *at the focal plane* of (+/- 2 lambda F# ^{2}). For a wavelength of 195 Angstroms and the nominal F-number of 403, this means a depth of focus of +/- 6.33 mm. The secondary mirror has a corresponding spacing range of (+/- 6.33 mm / (M^2 + 1)), where M is the magnification (8.054). This gives a secondary mirror spacing tolerance of +/- 0.096 mm.

The tilt tolerance can be derived geometrically by calculating the rotation of the secondary mirror about its vertex required to compensate for a small field angle change. Doing this for the HIREX on-axis geometry gives the ratio

(secondary mirror tilt) / (object space repointing) = 3.47

Thus the secondary mirror tilt tolerance is equal to (3.47) times the object space pointing stability requirement, which in turn would most likely be derived from pixel size considerations. Note that the conventional Airy diffraction limit defined by (2.44 lambda / D), where D is the diameter of the primary mirror, is equal to 0.016 arc-second for a wavelength of 195 Angstroms.